Structure and Physical Properties of Copper Thiomolybdate Complex, $(^nBu_4N)_3[MoS_4Cu_3Cl_4]$

Bok-Kyu Shin and Jaehong Han*

Metalloenzyme Research Group and Department of Biotechnology, Chung-Ang University, Anseong 456-756, Korea
**E-mail: jaehongh@cau.ac.kr*
Received August 29, 2008

Key Words : Cluster, Copper, Metal-chalcogenide, Thiomolybdate, X-ray structure

Transition metal-chalcogenide clusters have been extensively studied because of its relevance to biological interests and industrial applications.[1] For examples, biological nitrogen fixation is made possible by nitrogenase which contains FeMo cofactor (*R*-homocitrate-$MoFe_7S_9X$ (X = unknown) cluster)[2] and biological hydrogen gas production is catalyzed by hydrogenases which contain Fe_4S_4-Fe_2S_2 or Fe_4S_4-$FeNiS_2$ cluster in the active site.[3] Industrially, transition metal-chalcogenide clusters were synthesized as advanced materials for catalyses,[4] nonlinear optics,[5,6] and nanotechnology.[7]

Due to the structural relevance to nitrogenase FeMo cofactor, chemical reactivity of $(Cl_4\text{-cat})_2Mo_2Fe_6S_8(PR_3)_6$ (R = ethyl, propyl) (**I**) has been studied extensively (Figure 1).[8,9] The $Mo^{IV}_2Fe^{II}_6S_8$ core of **I** was the first example of Mo-Fe-S clusters with fully reduced Fe centers, and unique with the edge-shared two cuboidal $MoFe_3S_4$ units in the absence of other bridging ligand. Besides, short M-M distances in **I** were close to those found in the FeMo cofactor. The average Mo-Fe and Fe-Fe distances were found at 2.677(5) Å and 2.639(2) Å, respectively, and shortest among the Mo-Fe-S clusters. Inspired by the interactions between the FeMo cofactor and diatomic molecules, high pressure CO reaction with **I** was tried, and a series of Roussin-type sulfur-void cuboidal $MoFe_3S_3$ complexes was synthesized.[10,11] High pressure CO reactions of other Mo-Fe-S clusters also produced many organometallic-inorganic hybrid clusters,[12] including the unprecedented high nuclear $Fe(DMF)Cl(Cl_4\text{-cat})_2Mo_2Fe_2S_4(PEt_3)_2ClFe_4S_4(PEt_3)_3(CO)_6Cl$ complex.[13]

Ligand substitution reaction of **I** (R = propyl) with X (X = N_3^-, BH_4^-, Cl^-) resulted in the corresponding $[(Cl_4\text{-cat})_2(PPr_3)_2Mo_2Fe_6S_8X_4]^{2-}$ and $[(Cl_4\text{-cat})_2(PPr_3)_2Mo_2Fe_6S_8(PPr_3)_2X_2]^{2-}$ complexes.[14] Recently, reaction of **I** with thiophilic Cu(I) ion, $[Cu(MeCN)_4](PF_6)$, has produced various metal-substituted high-nuclearity Mo-Cu-Fe clusters.[15] At

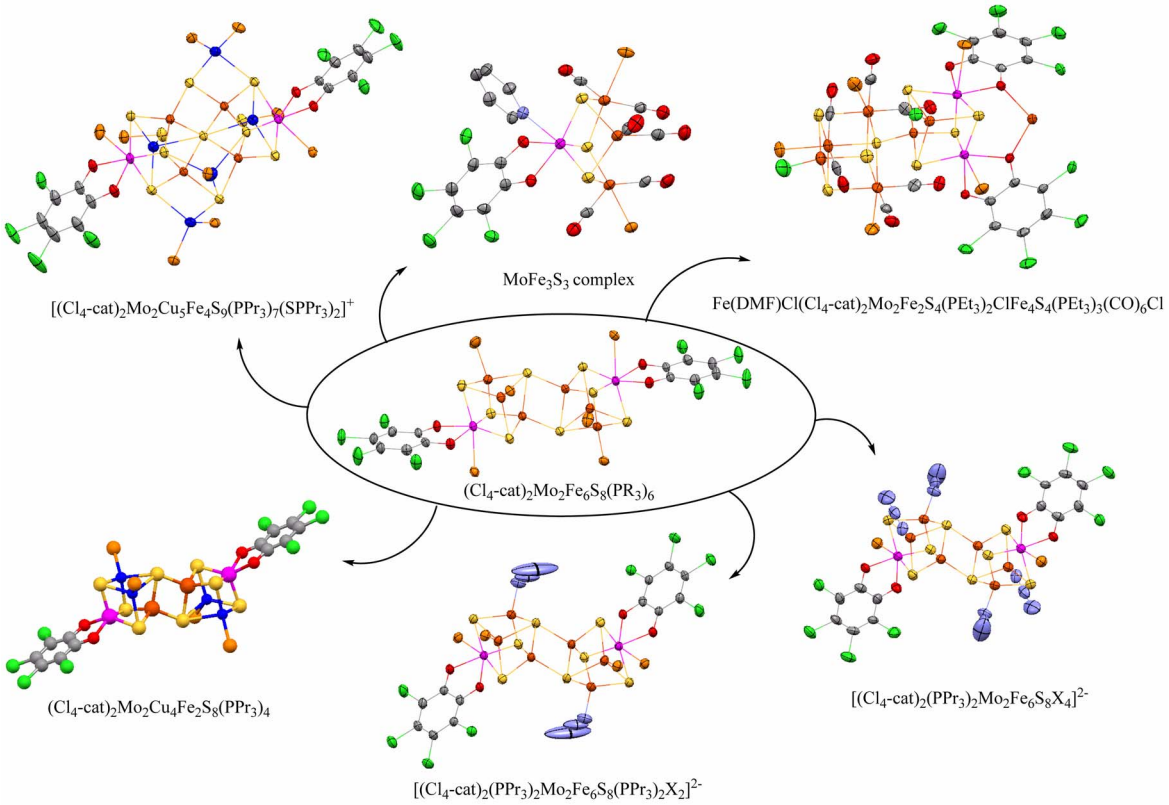

Figure 1. Chemical reactivity of $(Cl_4\text{-cat})_2Mo_2Fe_6S_8(PR_3)_6$ (R = ethyl, propyl).

low temperature, four iron center of **I** was substituted by four copper ions and isostructural $(Cl_4\text{-cat})_2Mo_2Cu_4Fe_2S_8(P^nPr_3)_4$ complex was synthesized.[15] On the contrary, complete rearrangement of the core structure was observed from the high temperature reaction, and the $[(Cl_4\text{-cat})_2Mo_2Cu_5Fe_4S_9(P^nPr_3)_7(SP^nPr_3)_2]PF_6$ complex was isolated.[16]

We have synthesized Mo-Fe-S cluster as a model complex of FeMo cofactor to understand its unique structural features.[17-19] Especially, an extensive M-M bonding framework related to the catalytic mechanism of N_2 reduction was investigated.[20] We have also shown that the extensive M-M bonding in the FeMo cofactor is due to the coordinative unsaturation of the metal centers.[21] Inspired by the recent preparation of Mo-Cu-Fe-S clusters, we have set out reactivity study of **I** with cupric ion, and isolated a new $(^nBu_4N)_3[MoS_4Cu_3Cl_4]$ (**II**) cluster from the reaction between **I** and $CuCl_2$. Although preparation of $MoCu_3(\mu_3\text{-}S)_3(\mu_3\text{-}Cl)$ cuboidal core from tetrathiomolybdate has been reported,[22] our work extends the chemical reactivity of **I** and the crystallographic structure and physical properties of **II** have never been reported. Here we report X-ray crystallographic structure and physical properties of the $(^nBu_4N)_3[MoS_4Cu_3Cl_4]$ (**II**) cluster.

The $(Cl_4\text{-cat})_2Mo_2Fe_6S_8(PEt_3)_6$ complex was reacted with $CuCl_2$ in the presence of tetrabutylammonium chloride. The solution changed its color to dark red during the reaction, and red rhombic crystalline products were isolated after ether layering. The IR spectrum of the product was almost same as that of $(^nBu_4N)_2[Fe_4S_4Cl_4]$ except the peaks at 497 cm^{-1} and 346 cm^{-1} due to the same counter cation, $^nBu_4N^+$. It is well documented the typical absorptions for the Mo-S stretching are found in the range of 400-500 cm^{-1}.[23] Mo=O stretching vibrations are known to be observed at around 910 cm^{-1} and complex **II** didn't show any peaks at the region. Generally, Mo-S stretching energy decreases as the coordination number of sulfide increases.[24] Thus, the IR absorption peaks of **II** at 497 cm^{-1} and 436 cm^{-1} were assigned to the ν(Mo-S_t) and ν(Mo-S_b), respectively.[25] The ν(Mo-S_t) of **II** at 497 cm^{-1} was higher than that of $[MoS_4]^{2-}$ at 463 cm^{-1}. Because Mo-S_t bonds of $[MoS_4]^{2-}$ is weakened by electrostatic repulsion, the Mo-S_t bond of **II** appears stronger than that of $[MoS_4]^{2-}$. Mircoprobe analysis clearly showed the absence of Fe atom, and the result suggested one Mo atom, three Cu atom and four S and Cl atoms in the crystals. CHN analysis suggested molecular formula of $(^nBu_4N)_3[MoS_4Cu_3Cl_4]$ and the structure was finally elucidated by X-ray crystallography (Table 1 and Figure 2).

The core structure of $(^nBu_4N)_3[MoS_4Cu_3Cl_4]$ (**II**) can be described as a distorted cube in which four corners are occupied by one Mo and three Cu atoms (with a chloride terminal ligand bonded to each Cu), and the other four corners are occupied by one μ_3-Cl atom and three μ_3-S atoms. Selected bond distances and angles are listed in Table 2. The unique Mo(1)-S(1) bond distance of **II** is 2.261(3) Å and which is slightly longer than 2.196(9) Å of $MoS_4Cu_3Cl(bipy)_2$,[26] and much longer than 2.036(2) Å of $MoS_4Cu_3(PyPPh_2)_3Cl$.[27] Typical bond distances for Mo-S_{br} are found in the range of 2.25-2.28 Å. The distances of Mo(1)-S(2), Mo(1)-S(3), and Mo(1)-S(4) are found at 2.2914(16) Å, 2.3354(16) Å, and 2.2378(16) Å, respectively, with a average value of 2.281(3, 4) Å. The average Mo-S distance of $(^nPr_4N)_2[MoS_4]$[28] is found at 2.1891(19, 4) Å,[29] and it appears the Mo-S bonds of **II** was elongated due to the complex formation. The distances between Cl(1) and other Cu centers are unequal. The weak interaction between Cu(3) and Cl(1) atoms are evident from the longest distance of 2.495(2) Å.

UV-Vis spectrum of **II** in MeCN is characterized by three strong absorptions at 329 nm, 368 nm and 503 nm (Figure

Table 1. Crystal data and structure refinement for $(^nBu_4N)_3[MoS_4Cu_3Cl_4]$

Empirical formula	$C_{48}H_{108}Cl_4Cu_3MoN_3S_4$
Crystal system, space group	Monoclinic, C*c*
Unit cell dimensions	a = 26.773(3) Å, b = 16.7446(18) Å, c = 15.8015(17) Å, β = 121.1710(10)°
Volume	6061.1(11) $Å^3$
Z, Calculated density	4, 1.407 Mg/m^3
Absorption coefficient	1.407 mm^{-1}
F(000)	2712
R(int)	0.0454
Data / restraints / parameters	17090 / 2 / 580
Goodness-of-fit on F^2	1.115
Final R indices for I > 2sigma(I) (all data)	R1 = 0.0841 (0.0856), wR2 = 0.1847 (0.1859)

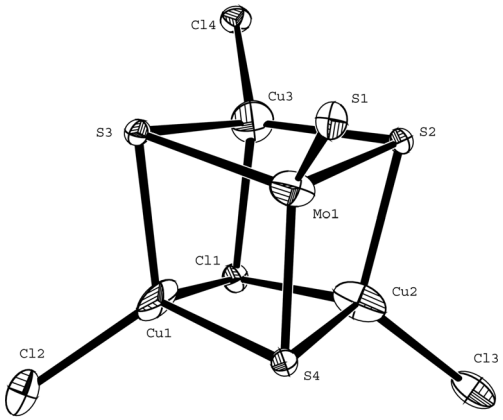

Figure 2. Crystallographic structure of $[MoS_4Cu_3Cl_4]^{3-}$ with thermal ellipsoids (50% probability).

Table 2. Selected bond lengths [Å] and angles [°] for $(^nBu_4N)_3[MoS_4Cu_3Cl_4]$

Cu(1)-Cl(2)	2.244(2)	S(4)-Mo(1)-S(2)	107.12(6)
Cu(1)-S(4)	2.2464(16)	S(4)-Mo(1)-S(3)	105.79(6)
Cu(1)-S(3)	2.3326(17)	S(2)-Mo(1)-S(3)	104.24(6)
Cu(1)-Cl(1)	2.4616(19)	S(4)-Cu(1)-S(3)	105.61(6)
Cu(2)-Cl(3)	2.250(2)	S(4)-Cu(1)-Cl(1)	102.13(6)
Cu(2)-S(2)	2.3370(17)	S(3)-Cu(1)-Cl(1)	99.21(6)
Cu(2)-Cl(1)	2.4182(18)	S(4)-Cu(2)-S(2)	105.21(6)
Cu(3)-Cl(4)	2.2042(17)	S(2)-Cu(3)-S(3)	101.06(6)
Cu(3)-S(2)	2.3515(18)	S(2)-Cu(3)-Cl(1)	97.78(6)
Cu(3)-Cl(1)	2.495(2)	S(3)-Cu(3)-Cl(1)	97.04(6)

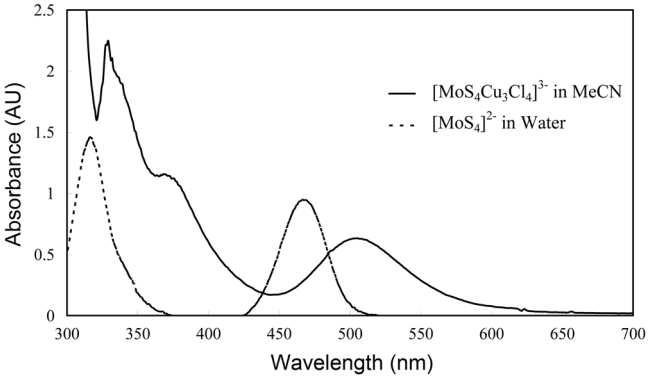

Figure 3. UV-Vis spectrum of **II** in MeCN.

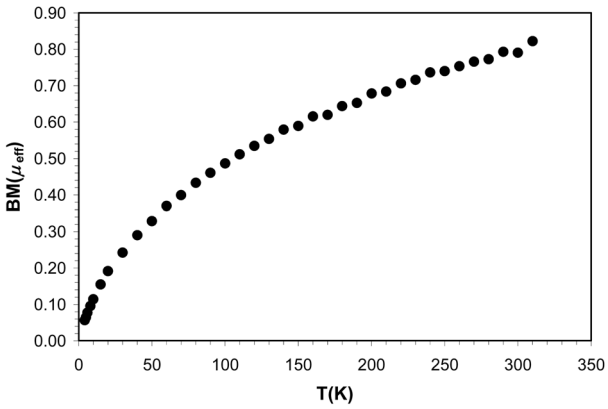

Figure 5. Temperature-dependent magnetic susceptibility of **I**.

3), which is due to the S → Mo charge transfer transitions. The free $[MoS_4]^{2-}$ anion in water shows strong absorptions at 241 nm, 316 nm and 467 nm. The electronic transitions of **II** were red-shifted, which can be explained based on the structural information. The average Mo-S distance of **II** is about 0.1 Å longer that that of $[MoS_4]^{2-}$, and the weakening of Mo-S bonds has possibly contributed lower energy electronic transitions of **II**.

The cyclic voltammetry of the $(^nBu_4N)_3[MoS_4Cu_3Cl_4]$ (**II**) complex showed multi-redox waves (Figure 4). Two quasi-reversible oxidation waves at E_{pc1} = 0.80 V and E_{pc2} = 1.16 V versus Ag/AgCl can be assigned to the oxidation of Cu(I) centers, and two reduction waves at E_{pa1} = −1.20 V and E_{pa2} = −1.78 V can be assigned to the successive reduction of Mo(VI) center.[30] The formal oxidation states of the metal centers at the $[MoCu_3]^{9+}$ core can be formalized as $Mo^{VI}Cu^{I}_3$, based on the literatures.[31,32] It is known that the $MoCu_3$ clusters are diamagnetic due to the d^0 (Mo^{VI}) and d^{10} (Cu^{I}) electronic configurations. The magnetic susceptibilities of $(^nBu_4N)_3[MoS_4Cu_3Cl_4]$ (**II**) were measured over various temperatures at 5000 G. The complex **II** showed μ_{eff} = 0.82 BM at 310 K and μ_{eff} = 0.06 BM at 4.2 K. Temperature-dependent magnetic susceptibility measurement of **II** is shown at Figure 5. Unlike expected, the $(^nBu_4N)_3[MoS_4Cu_3Cl_4]$ (**II**) complex showed paramagnetic property with anti-ferromagnetic exchange coupling interactions. It appear to us the $(^nBu_4N)_3[MoS_4Cu_3Cl_4]$ (**II**) complex is, at least partially, a mixed-valence system with a $Mo^{V}Cu^{I}_2Cu^{II}$ characteristics.

In summary, we have synthesized the $(^nBu_4N)_3[MoS_4Cu_3Cl_4]$ (**II**) complex from the reaction between $(Cl_4\text{-cat})_2Mo_2Fe_6S_8(PEt_3)_6$ and $CuCl_2$ in the presence of $^nBu_4NCl$. The X-ray crystallographic structure of **II** has been determined and the physical properties of vibrational and electronic transitions, redox potentials, and temperature-dependent magnetic susceptibility, have been studied.

Experimental Section

General. All experiments and reactions were carried out under a dinitrogen atmosphere with standard Schlenk line techniques or in an inert atmosphere glovebox. All solvents were distilled under dinitrogen and nitrogen gas was bubbled through each before use.[33] Acetonitrile was predried over oven-dried molecular sieves and distilled over CaH_2. $CuCl_2$ and $^nBu_4NCl$ were purchased from Aldrich and used for the reaction without further purification. $(Cl_4\text{-cat})_2Mo_2Fe_6S_8(PEt_3)_6$,[8,9] and $(NH_4)[MoS_4]$[34] were prepared according to published methods.

UV-Vis spectra were recorded on a Scinco-3100 UV-Visible spectrophotometer. FT-IR spectra were collected on a Shimadzu FT-IR 8400S FT-IR spectrometer in KBr pellets and the spectra were corrected for background. Elemental analyses were performed in the Stable Isotope Laboratory at NICEM (Seoul, Korea). The data were adjusted by using acetanilide as a standard. Cyclic voltammetry experiments were carried out by a Princeton Applied Research model 263A Potentiostat with a K0264 microcell kit. Three electrodes, consisting of a glassy carbon working electrode,

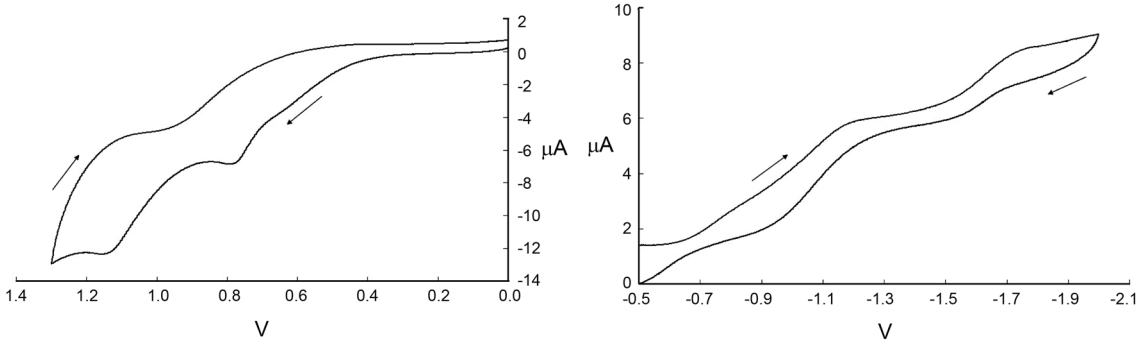

Figure 4. Cyclic voltammetric responses of $(^nBu_4N)_3[MoS_4Cu_3Cl_4]$ (**II**) in MeCN.

a Pt auxiliary electrode and a silver/silver chloride electrode (Ag/AgCl) as a reference electrode, were used for the measurements. The potentials are reported *vs* Ag/AgCl as a reference electrode with use of 0.1 M of (nBu_4N)(PF_6) as supporting electrolyte. The scanning rate was 50 mV/s and $E_{1/2}$ of the ferrocene oxidation in MeCN was observed at +0.455 V under these conditions.

($^nBu_4N$)$_3$[$MoS_4Cu_3Cl_4$] (II). The $(Cl_4\text{-cat})_2Mo_2Fe_6S_8(PEt_3)_6$ cluster (500 mg, 0.25 mmol) was suspended in 25 mL of MeCN, and $CuCl_2$ (100 mg, 0.72 mmol) and $^nBu_4NCl$ (100 mg, 0.35 mmol) were added. The reaction was set to reflux for 2 hours and then filtered to remove black precipitates. To the filtrate, 50 mL of ether was layered over the solution to induce incipient crystallization. After several days, a total of 200 mg of dark red crystals was isolated (0.156 mmol, yield 31%, based on Mo). ($^nBu_4N$)$_3$[$MoS_4Cu_3Cl_4$] FT-IR (KBr, cm^{-1}) ($^nBu_4N$); 2959 (s), 2873 (m), 1480 (s), 1383 (m), 880 (m) 733 (m), ν(Mo-S_t); 497 (s), ν(Mo-S_b); 436 (s). Anal. Calcd for $C_{48}H_{108}Cl_4Cu_3MoN_3S_4$ (MW 1284.04): C, 44.90; H, 8.48; N, 3.27. Found: C, 46.73; H, 8.75, N, 3.33. UV-Vis (purple in MeCN): λ_{max} (ε) = 329 nm (749 $mM^{-1}cm^{-1}$), 368 nm (384 $mM^{-1}cm^{-1}$), 503 nm (214 $mM^{-1}cm^{-1}$). Magnetic susceptibility: 0.79 μ_B (300 K), 0.06 μ_B (4 K).

X-ray Crystallography. Dark red rhombic crystals of ($^nBu_4N$)$_3$[$MoS_4Cu_3Cl_4$] were obtained from the mother liquor by solvent diffusion after several days. The diffraction data was collected at 85(2) K using a Bruker SMART area diffractometer equipped with a monochromator in the Mo Kα (λ = 0.71073 Å) incident beam. The CCD data were integrated and scaled using the Bruker-SAINT software package,[35] and the structure was solved and refined using SHEXTL V5.10.[36] The crystal data and structural parameters are shown in Tables 1 and Table 2. The structure was solved by direct methods to locate heavy atoms, and the nonhydrogen atoms were located through subsequent difference Fourier syntheses. Structural refinement was carried out by full-matrix least squares on F^2. All non-hydrogen atoms were refined with anisotropic thermal parameters. Hydrogen atoms were located in the calculated positions.

Acknowledgments. This work was supported by the Korean Research Foundation Grant (KRF-2006-331-F00015) funded by the Korean Government (MOEHRD). This research was also partially supported by the Chung-Ang University Excellent Researcher Grant in 2008.

Supplementary data. Crystallographic data for the structure reported here have been deposited with Cambridge Crystallographic Data Center (Deposition No. CCDC 684991). The data can be obtained free of charge *via* www.ccdc.cam.ac.uk/conts/retrieving.html (or from the CCDC, 12 Union Road, Cambridge CB2 1EZ, UK; fax: +44 1223 336033; e-mail: deposit@ccdc.cam.ac.uk).

References

1. Stiefel, E. I.; Matsumoto, K. *Transition Metal Sulfur Chemistry: Biological and Industrial Significance*; American Chemical Society: Washington DC, 1996.
2. Einsle, O.; Tezcan, A. F.; Andrade, S. L. A.; Schmid, B.; Yoshida, M.; Howard, J. D.; Rees, D. C. *Science* **2002**, *297*, 1696-1700.
3. Best, S. P. *Coord. Chem. Rev.* **2005**, *249*, 1536-1554.
4. Park, D.-S.; Jabbar, M. A.; Park, H.; Lee, H. M.; Shin, S.-C.; Shim, Y.-B. *Bull. Korean Chem. Soc.* **2007**, *28*, 1996-2002.
5. Tan, W. L.; Zheng, H. G.; Jin, Q. H.; Jin, G. C.; Ji, W.; Long, V.; Xin, X. Q. *Polyhedron* **2000**, *19*, 1545.
6. Zhang, C.; Song, Y.; Kühn, F. E.; Wang, Y.; Xin, X.; Herrmann, W. A. *Adv. Mater.* **2002**, *14*, 818-822.
7. Kwon, S. G.; Hyeon, T. *Acc. Chem. Res*. **2008**, ASAP Articles, ar8000537.
8. Demadis, K. D.; Campana, C. F.; Coucouvanis, D. *J. Am. Chem. Soc*. **1995**, *117*, 7832-7833.
9. Han, J.; Koutmos, M.; Ahmad, S. A.; Coucouvanis, D. *Inorg. Chem*. **2001**, *40*, 5985-5999.
10. Han, J.; Beck, K.; Ockwig, N.; Coucouvanis, D. *J. Am. Chem. Soc*. **1999**, *121*, 10448-10449.
11. Coucouvanis, D.; Han, J.; Moon, N. *J. Am. Chem. Soc*. **2002**, *124*, 216-224.
12. Han, J.; Huang, M.; Coucouvanis, D. *Polyhedron* **2002**, *21*, 2523-2530.
13. Han, J.; Coucouvanis, D. *J. Am. Chem. Soc*. **2001**, *123*, 11304-11305.
14. Koutmos, M.; Georgakaki, I. P.; Coucouvanis, D. *Inorg. Chem*. **2006**, *45*, 3648-3656.
15. Koutmos, M.; Coucouvanis, D. *Angew. Chem. Int. Ed*. **2005**, *44*, 1971-1974.
16. Koutmos, M.; Coucouanis, D. *Inorg. Chem*. **2006**, *45*, 1421-1423.
17. Han, J.; Coucouvanis, D. *Dalton Trans*. **2005**, 1234-1240.
18. Han, J.; Nam, W. *Bull. Korean Chem. Soc*. **2004**, *25*, 910-912.
19. Shin, B.-K.; Han, J. *Bull. Korean Chem. Soc*. **2006**, *27*, 17-18.
20. Han, J.; Newton, W. E. *Biochemistry* **2004**, *43*, 2947-2956.
21. Kim, M.; Han, J. *Polyhedron* **2007**, *26*, 2949-2956.
22. Jeannin, Y.; Sécheresse, F.; Bernès, S.; Robert, F. *Inorg. Chim. Acta* **1992**, *198-200*, 493-505.
23. Müller, A.; Diemann, E.; Jostes, R.; Bögge, H. *Angew. Chem. Int. Ed. Engl*. **1981**, *20*, 934-955.
24. Zhang, C.; Jin, G. C.; Chen, J. X.; Xin, X. Q.; Qian, K. P. *Coord. Chem. Rev.* **2001**, *213*, 51-77.
25. Shen, J.-K.; Gao, Y.-C.; Shi, Q.-Z.; Basolo, F. *Inorg. Chem*. **1989**, *28*, 4304-4306.
26. Zhou, J.-L.; Li, Y.-Z.; Zheng, H.-G.; Xin, X.-Q. *Trans. Met. Chem.* **2004**, *29*, 185-188.
27. Cai, Y. A.; Zheng, H.; Li, Y.; Zhou, J.; Song, Y.; Xin, X. *J. Coord. Chem*. **2003**, *56*, 595-601.
28. Unpublished results.
29. Mean values of crystallographically independent and chemically equivalent structural parameters. The number in parenthesis represents the larger of the individual standard deviations or the standard deviation from the mean σ = SQRT{$\Sigma(x_i-\bar{x})^2/n(n-1)$}. n = number of parameter.
30. Guo, J.; Sheng, T.; Zhang, W.; Wu, X.; Lin, P.; Wang, Q.; Lu, J. *Inorg. Chem*. **1998**, *37*, 3689-3697.
31. Müller, A.; Bögge, H.; Tölle, H.-G.; Jostes, R.; Schimanski, U.; Dartmann, M. *Angew. Chem. Int. Ed. Engl*. **1980**, *19*, 654-655.
32. Hou, H.; Ye, X.; Xin, X.; Liu, J.; Chen, M.; Shi, S. *Chem. Mater*. **1995**, *7*, 472-476.
33. Shin, B.-K.; Kim, M.; Han, J. *Bull. Korean Chem. Soc.* **2007**, *28*, 417-420.
34. McDonald, J. W.; Friesen, G. D.; Rosenhein, L. D.; Newton, W. E. *Inorg. Chem. Acta* **1983**, *72*, 205-210.
35. Bruker *SMART and SAINT*; Bruker AXS Inc.: Madison, Wisconsin, USA, 1997.
36. Bruker *SHELXTL*, Version 5.10; Bruker AXS Inc.: Madison, Wisconsin, USA, 1998.